

Remarkable signals of t_R compositeness

G.J. Gounaris^a and F.M. Renard^b

^aDepartment of Theoretical Physics, Aristotle University of Thessaloniki,
Gr-54124, Thessaloniki, Greece.

^bLaboratoire Univers et Particules de Montpellier, UMR 5299
Université Montpellier II, Place Eugène Bataillon CC072
F-34095 Montpellier Cedex 5, France.

Abstract

We are looking for remarkable differences between predictions of the standard model and those of t_R compositeness (while the t_L remains elementary) in various basic $t\bar{t}$ production processes, without having to make difficult final polarization analyses. We assume the presence of q^2 dependent form factors which first suppress the t_R contributions at high q^2 , and in addition, may also lead to an effective q^2 dependent top mass. We further assume that these effects disappear at low q^2 , so that there are no anomalous couplings. We show that large specific differences indeed appear in the high energy limits of cross sections and asymmetries in e^-e^+ , gluon+gluon, $\gamma\gamma$ collisions and other fusion processes and that this should lead to a strategy for analyzing them.

PACS numbers: 12.15.-y, 12.60.-i, 14.65.Ha, 14.80.-j

1 INTRODUCTION

Motivated by several deficiencies of SM, the possibility of compositeness of particles previously considered as elementary has been considered since a long time [1]. This idea has been applied to the Higgs sector and it has also been assumed that a new world directly related to the Higgs boson and connected to the ordinary fermions could be at the origin of the fermion masses. The top quark, with its heavy mass, would be especially concerned by this feature. The broad spectrum of fermionic masses has suggested the possibility of partial compositeness where the size of the mixing of an elementary fermion with a corresponding new state is related to the value of its mass. The high mass of the top quark would correspond to a large mixing value and even to the full t_R compositeness. The t_L state would remain elementary in order to not perturb the (pure left) Wtb system. Models based on these assumptions have already appeared, see for example [2, 3, 4, 5].

We do not intend to analyze such models in details but we want to suggest basic and quick tests of the appealing idea that t_R would be composite, whereas t_L would remain elementary. We then show in which processes and through which observables these basic tests could be performed, without making a difficult final polarization analysis. Indeed, we will find places where spectacular differences should appear between the usual elementary top case and the above composite t_R , elementary t_L , case.

Our basic point is that a composite t_R should have a form factor $F(q^2)$ such that its production through photon, Z, gluon point-like couplings should be suppressed at high q^2 . On the opposite, the elementary t_L will keep the usual Born coupling (with obviously higher order, small corrections that we do not consider at this level of the study). The pure left W couplings will not be modified. The Higgs couplings (connecting t_R and t_L) are particularly model dependent and several types of modifications may appear. Among them we will introduce the concept of effective top mass in processes where the value of the top mass controls the behaviour of the amplitudes at high energy, for example in those involving Higgs boson or longitudinal W, Z .

We apply these considerations to several $t\bar{t}$ production processes in e^-e^+ , gluon-gluon, $q\bar{q}$, $\gamma\gamma$, WW , ZZ collisions, as well as in single top production. The high energy limits of their observables are computed in different options and indeed in some cases they lead to spectacular differences (simple factors) between the SM and the composite t_R case, which could be observable without making difficult final polarization measurements.

We insist on the basic aspect of our note: we are not discussing the existence of anomalous couplings (their possible measurements at LHC and ILC are for example discussed in [6, 7]), but the presence of q^2 dependent form factors, which do not modify the SM couplings at low q^2 ; they would modify the t_R production at high q^2 but not the t_L one. In the following, we make illustrations using arbitrary test-form factors, just in order to show how these high energy limits may be reached. More detailed special studies and experimental tests could be done in the spirit of [8, 9].

The organization of the paper is the following. The $e^-e^+ \rightarrow t\bar{t}$ process is treated in Sec. II, $gg \rightarrow t\bar{t}$ and other hadronic processes in Sec. III, photon-photon collision, WW and ZZ fusion and other processes in Sec. IV. Conclusions and possible developments are

given in Sec. V.

2 $e^-e^+ \rightarrow \gamma, Z \rightarrow t\bar{t}$

We modify the usual SM point-like Vtt ($V = \gamma, Z$) as

$$\bar{u}_t\gamma^\mu[g_{Vt}^L P_L + g_{Vt}^R P_R]v_t \rightarrow \bar{u}_t\gamma^\mu[g_{Vt}^L P_L + g_{Vt}^R P_R F(s)]v_t \quad , \quad (1)$$

where $P_{L/R} = (1 \mp \gamma^5)/2$, the t_L is kept elementary with its SM point-like couplings, while the t_R compositeness introduces a form factor through the replacement

$$g_{Vt}^R \rightarrow g_{Vt}^R F(s) \quad , \quad (2)$$

which for the consistency of the theory it is assumed to hold not only for $V = \gamma, Z$, but for the gluon also. In the numerical illustration we use the "test-form factor"

$$F(s) = \frac{4m_t^2 + M^2}{s + M^2} \quad , \quad (3)$$

where M is a new physics scale fixed at 0.5 TeV in the illustration. Thus, $F(s)$ is equal to 1 at threshold and tends to 0 at high energy. Our aim is to emphasize the high energy properties when the t_R contribution is suppressed. No special meaning is given to the precise form factor expression. A global change of scale could be easily done if one wants to discuss the observability at a very high energy collider.

The various observables (polarized, unpolarized cross sections and asymmetries) are then computed with the usual formulas (see for example [10]). The observability of anomalous electroweak couplings in such processes has been recently discussed in [6, 11]. But we now consider the ratios of the values of the observables in the composite t_R case over the ones in the standard case. We want to emphasize the leading effects of t_R compositeness, from the fact that it may imply (contrarily to the t_L contribution) that its corresponding photon and Z couplings are suppressed at high energy, by progressively vanishing above the new physics scale. At this stage of the study, we ignore the 1 loop and higher order QCD or electroweak corrections. These corrections affect slightly the absolute values, but should not sensibly modify the ratios.

As one can see in Figure 1 , at high energy, (say above 1 TeV for $M = 0.5\text{TeV}$) we obtain the following values for the above mentioned ratios:

- 0.61 for the total unpolarized cross section ratios σ_{unp} ,
- 0.88 for the longitudinally polarized cross section ratio σ_{long} ,
- 0.67 for the transverse polarization azimuthal factor σ_{trans} ,
- 1.17 for the unpolarized forward-backward asymmetry A_{unp}^{FB} ,

- a longitudinally polarized forward-backward asymmetry A_{long}^{FB} , varying in the range (1.25-2.25),
- and 2.81 for the longitudinal polarization asymmetry A_{long}^{pol} .

One can see that the most spectacular effects are already present in the total unpolarized cross section, but also in the longitudinal e^-e^+ polarization asymmetry, as well as in the azimuthal distribution in the case of transverse e^-e^+ polarization and the unpolarized forward-backward asymmetry.

Similar effects should be observed in $\mu^+\mu^- \rightarrow t\bar{t}$. This process only differs by the presence of the Higgs exchange in the s-channel but this contribution is too weak to modify substantially the above results.

3 EFFECTS IN HADRONIC COLLISIONS

The main $t\bar{t}$ production mechanism is now $gg \rightarrow t\bar{t}$. At tree level there are 3 diagrams: (a) s-channel gluon exchange, (b) top exchange in the t-channel, (c) top exchange in the u-channel. For recent analyses of this process with high order corrections see e.g. [12] and for the search of anomalous couplings see [7]. In our framework, we modify the t_R couplings with the form factor $F(s)$ in (a), $\tilde{F}(t)$ in (b) and $\tilde{F}(u)$ in (c). Thus the total Born amplitude is written as

$$A^{Born} = A^{Born\ a} + A^{Born\ b} + A^{Born\ c} \ , \quad (4)$$

with the three terms respectively given by

$$A^{Born\ a} = -if^{ijl} \frac{\lambda^l}{2} \frac{4\pi\alpha_s}{s} (\epsilon.\epsilon') \left[\bar{u}_t \gamma^\mu (k - k')_\mu \left(P_L + F(s) P_R \right) v_t \right] \ , \quad (5)$$

$$A^{Born\ b} = - \frac{4\pi\alpha_s}{t - m_t^2} \frac{\lambda^i \lambda^j}{2} \bar{u}_t \left[\gamma^\mu \epsilon_\mu \gamma^\nu (p - k)_\nu \gamma^\rho \epsilon'_\rho \left(P_L + \tilde{F}^2(t) P_R \right) + m_t \gamma^\mu \epsilon_\mu \gamma^\rho \epsilon'_\rho \tilde{F}(t) \right] v_t \ , \quad (6)$$

$$A^{Born\ c} = - \frac{4\pi\alpha_s}{u - m_t^2} \frac{\lambda^j \lambda^i}{2} \bar{u}_t \left[\gamma^\mu \epsilon'_\mu \gamma^\nu (p - k')_\nu \gamma^\rho \epsilon_\rho \left(P_L + \tilde{F}^2(u) P_R \right) + m_t \gamma^\mu \epsilon'_\mu \gamma^\rho \epsilon_\rho \tilde{F}(u) \right] v_t \ , \quad (7)$$

where the initial gluons have color indices (i, j) , momenta (k, k') , polarization vectors (ϵ, ϵ') , while p denotes the momentum of the final t -quark and $P_{L/R}$ have already been defined immediately after (1).

Precise prediction for the energy behaviour of this cross section will depend on the choice of t_R form factors $F(s)$ and $\tilde{F}(t)$, $\tilde{F}(u)$, where one should use (3) for $F(s)$, while

for a virtual top in the t or u channel we should use

$$g_{Vt}^R \rightarrow g_{Vt}^R \tilde{F}(x) \quad , \quad (8)$$

$$\tilde{F}(x) = \frac{M^2}{-x + M^2} \quad , \quad x = t, u \quad . \quad (9)$$

Doing so, we obtain in the central region the results shown in Figure 2, where we give the ratio of the modified cross section over the standard one. The curve is drawn for $\theta = \frac{\pi}{2}$ but it is valid for any other central value, as soon as the corresponding t, u values are comparable to s .

This ratio should not be sensibly affected by QCD corrections. As already mentioned such an arbitrary choice of form factor has no special meaning, we just want to insist on the fact that, at high energy, the t_R contribution which was equal to the t_L one in SM (apart from small differences due to electroweak corrections) is suppressed by the form factors. As one can see in Figure 2 this suppression leads indeed quickly to a reduction of the cross section by a factor 1/2.

4 FUSION AND OTHER PROCESSES

4.1 $\gamma\gamma \rightarrow t\bar{t}$.

Here we assume that real photon-photon collisions will be observable at future colliders; for recent studies see [15]. The basic process is similar to gluon-gluon process $gg \rightarrow t\bar{t}$ considered in Sec. III, except for the absence of the s-channel term. In analogy to (6, 7), the t - and u - channel terms are respectively given by

$$A^{Born\ b} = -\frac{e^2 Q_t^2}{t - m_t^2} \bar{u}_t \left[\gamma^\mu \epsilon_\mu \gamma^\nu (p - k)_\nu \gamma^\rho \epsilon'_\rho \left(P_L + \tilde{F}^2(t) P_R \right) + m_t \gamma^\mu \epsilon_\mu \gamma^\rho \epsilon'_\rho \tilde{F}(t) \right] v_t \quad , \quad (10)$$

$$A^{Born\ c} = -\frac{e^2 Q_t^2}{u - m_t^2} \bar{u}_t \left[\gamma^\mu \epsilon'_\mu \gamma^\nu (p - k')_\nu \gamma^\rho \epsilon_\rho \left(P_L + \tilde{F}^2(u) P_R \right) + m_t \gamma^\mu \epsilon'_\mu \gamma^\rho \epsilon_\rho \tilde{F}(u) \right] v_t \quad (11)$$

where we use the same t_R form factors as above. The result for the ratio of differential cross sections in the central region (for large t, u) is also illustrated in Figure 2. As expected, we obtain also a reduction by a factor 1/2 at high energy, similarly to the $gg \rightarrow t\bar{t}$ case.

4.2 FUSION PROCESSES in e^+e^- OR HADRONIC COLLISIONS

We consider the $WW, ZZ, \gamma\gamma, \gamma Z \rightarrow t\bar{t}$ processes, for which basic studies can be found in [16, 17, 18, 19]. Specifically, we find:

- (a) For $WW \rightarrow t\bar{t}$.

In this process the t - and u -channel bottom exchanges with the left-handed W couplings have no form factor effect. The s -channel γ, Z exchange contributions though, could be sensitive to the t_R form factor, but at high energy the right-handed part of the $\gamma + Z$ contribution cancels (it corresponds to the pure left W^3 exchange). So finally the modifications will only arise from the s -channel Higgs exchange connecting t_L to t_R and being proportional to the top mass. This contribution is totally model dependent, and we will consider two extreme situations.

First, if this Higgs part retains its SM structure, the global $WW \rightarrow t\bar{t}$ amplitudes, dominated by the t_L parts, will be very similar to the standard case. In this case the ratio of cross sections to SM will be close to 1.

On the opposite, if we suppose that both the Higgs boson and the t_R are composite, whereas the t_L remains elementary and point-like, then one can expect that at high energy the Ht_Lt_R coupling will be suppressed by the same type of form factor effects which suppress the $\gamma t_R t_R$ and $Zt_R t_R$ couplings.

But this cannot be the only feature. The suppression of the $WW \rightarrow H \rightarrow t\bar{t}$ contribution will create a problem with the necessary cancellation of the increasing $W_L W_L$ amplitudes at high energy. Indeed at high energy in SM, the sum of the contributions due to γ, Z exchange in the s -channel and bottom exchange in the t and u channel is proportional to the top mass and is canceled by the H exchange in the s channel. The suppression of this last contribution should be accompanied by a suppression of the first sum. The simplest solution to this problem could be to replace the fixed value of the top mass by an effective mass (a kind of scale dependent mass in a way similar to the QCD case, but much more violent, being due to compositeness), i.e. in this picture we would replace the top mass as

$$m_t \rightarrow m_t(s) = m_t F(s) \quad . \quad (12)$$

This mass suppression affects both single and double longitudinal W_L contributions (that are proportional to the top mass) and together with the suppression of the Higgs exchange contribution leads to a strong reduction of the cross section, as one can see by comparing the left and right panels of Figure 3. Note that in the left panel only the g_{Vt}^R replacement effects (2, 8) are used, while in the right panel the m_t replacement (12) is also included. As shown in the right panel of Figure 3, at high energy the ratio becomes of the order of 0.2.

- (b) $ZZ \rightarrow t\bar{t}$

The t - and u -channel top exchanges now involve contributions from both t_L without form factor and t_R with its form factor. However the standard $Zt_R t_R$ coupling is already (about 2 times) weaker than the $Zt_L t_L$ one and as these couplings appear squared in these amplitudes (so at 4th power in the cross section), the suppression of the t_R coupling would produce almost no visible effect in the cross section. On

another hand the s -channel now only involves the Higgs exchange and requires the same study as in the above WW case.

Considering again the two above extreme cases (suppression of the t_R coupling with a minimal change of Higgs coupling or the same with, in addition, a suppressed effective top mass) we would obtain high energy ratio values of the order of 1 or of 0.7, respectively; see left and right panels of Figure 3 respectively. However this ZZ channel is not directly observable because one should add the $\gamma\gamma, \gamma Z$ background processes; these are indicated in the panels of Figure 3 as “ ZZ +back”.

- (c) $\gamma\gamma, \gamma Z \rightarrow t\bar{t}$

These subprocesses should be added to the ZZ one when considering $e^-e^+ \rightarrow e^-e^+ + t\bar{t}$. They do not involve tree level Higgs exchange, so they are less model dependent. Their t_R suppression effect is rather similar to what we have seen in the above real $\gamma\gamma$ case, leading to a reduction factor of the order of 0.5. However if we apply the effective top mass rule, the $Z\gamma$ and γZ channels which have a large Z_L contribution proportional to the top mass are strongly affected and this leads to a ratio of the order of 0.3.

The addition of these various transverse and longitudinal contributions to these four processes, with different energy dependencies, finally produces a ratio which is very sensitive to the details of the non standard effects. The relative importance of the background with respect to ZZ can be varied by applying angular cuts on the final e^-e^+ pair, but in any case, we find a global reduction factor respectively of the order of 0.5 for the t_R coupling suppression and of 0.4 when one adds the effective mass rule as one can see in the right panel Figure 3.

4.3 OTHER PROCESSES

We have seen that the main $t\bar{t}$ production processes in e^-e^+ , gluon-gluon, and $\gamma\gamma$ collisions are clearly and directly sensitive to the t_R form factor suppression. On another hand, we have seen that the WW , ZZ fusion processes are in addition also sensitive to the H compositeness structure and that this could lead to further suppression effects. We have considered the possibility of a (very important) scale dependent top mass $m_t(s)$ which strongly affects this fusion class of processes. But it would not affect the above main $t\bar{t}$ production processes (in e^-e^+ , gluon-gluon, and $\gamma\gamma$ collisions) because at high energy the top mass has a negligible effect in these processes.

We can also mention that other simple top production mechanisms like $q\bar{q} \rightarrow \gamma, Z, H \rightarrow t\bar{t}$ are less affected by the t_R form factor suppression at high energy, because of particular quark couplings combinations; while in $q\bar{q}' \rightarrow W \rightarrow t\bar{b}$ a similar consequence is induced by the high energy t_L -dominance, with the unmodified left-handed W coupling.

We have nevertheless considered the $bg \rightarrow tW^-$ process (see [13] for recent studies) for which the $(b_-g_+ \rightarrow t_R W_{long}^-)$ helicity amplitude, although involving the left-handed W coupling, is directly proportional to the top mass coming from the u-channel top exchange

(see [14]). This property can be understood by using the equivalence with the $bg \rightarrow tG^-$ and the Goldstone coupling proportional to m_t .

Applying the replacement (12) of m_t by the effective top mass, would have the effect of essentially suppressing this longitudinal W contribution at high energy. Adding the unaffected transverse W contributions, would then lead to a resulting total unpolarized $bg \rightarrow tW^-$ cross reduced by a factor 0.7 with respect to the SM case, in the central region at energies above 1 TeV; see Figure 4. Let us add that one should not forget that the Goldstone equivalence is only valid in gauge theories so that it may not apply to any kind of effective Higgs description.

There are however other more complex processes which are directly sensitive to the top mass. Such processes are:

- $e^-e^+ \rightarrow t\bar{t}H$.

This is the simplest one, whose Born contributions involve production of $t\bar{t}$ through γ, Z exchange in the s-channel and emission of H by t, \bar{t} , or the intermediate Z ; see [20]. Note that the first two cases involving the $Ht\bar{t}$ vertex, are directly sensitive to the top mass. Here again we look at the two possibilities, either the simple suppression of t_R couplings to γ, Z given by (2, 8) (keeping unchanged the standard $Ht\bar{t}$ couplings) or by imposing in addition the $m_t(s)$ suppression through (12). The results are shown in Figure 5, with the first option giving a reduction by a factor of just above 0.4, and the second one giving a stronger regular decrease.

- $e^-e^+ \rightarrow t\bar{t}Z$, studied in [21].

Here again the Born contribution is built by starting from the diagram $t\bar{t}$ production through γ, Z exchange in the s-channel, and inserting to it a Z -production vertex. We thus encounter the competition of two different kinds of diagrams: first, Z emission from t, \bar{t} lines (with γ, Z exchange in the s-channel) together with Z exchange in the s-channel with intermediate ZZH coupling followed by $H \rightarrow t\bar{t}$, which are very sensitive to the top properties in particular to the top mass; second, Z emission from e^-, e^+ lines (with γ, Z exchange in the s-channel which is the only part slightly sensitive to the t_R couplings). In Figure 6 we show both the unpolarized Z production and the longitudinal Z_L case with the same two options of t_R and $m_t(s)$ modifications, as above. Again one sees that Z_L production (from the first set) has a large sensitivity to the top mass due to its basic cancellation property (in agreement with Goldstone equivalence) but this effect is hidden at high energy by the terms coming from the second set which do not have this property.

- $gg, \gamma\gamma \rightarrow t\bar{t}H$ and $t\bar{t}Z$.

In order to explore more directly the final state properties (especially in the $t\bar{t}Z$ case) one should use another production process, for example in gluon-gluon or in $\gamma\gamma$ collisions which do not involve the above initial Z emission. In these cases the amplitudes correspond solely to t, u channel top exchange and (in the gluon-gluon

case) to s channel gluon exchange. So we have considered both $t\bar{t}H$ and $t\bar{t}Z$ production in the gluon-gluon and in the $\gamma\gamma$ cases. As above we have computed the two types of ratios of new cross sections over standard ones, the first one corresponding to gluon, γ and Z couplings to t_R being affected by the effective form factor, and the second type involving, in addition, the reduced effective top mass.

The results are illustrated in Figure 7-10. For simplicity we have computed the ratios of differential cross sections computed in the center of the 3-body phase space. They should be very close to ratios of integrated cross sections with cuts avoiding collinear domains. In the $t\bar{t}H$ case (Figure 7,8) one gets reduction effects similar or even stronger than the ones obtained in $e^+e^- \rightarrow t\bar{t}H$. In the $t\bar{t}Z$ case one gets also similar effects (Figure 9,10) again with the large sensitivity of Z_L production to the effective top mass. The pure transverse Z_T production is not shown because it is very little affected and especially not by the reduction of the effective top mass.

4.4 FINAL REMARK

One may finally worry about the possibility of partial t_R compositeness. In practice it means that the effective $\gamma t_R t_R$ and $Z t_R t_R$ couplings should be modified by a factor of the type

$$\cos \phi + F(s) \sin \phi \tag{13}$$

where ϕ is the mixing angle (which is equal to $\pi/2$ in the full compositeness case) of the elementary top quark with the new sector and $F(s)$ a form factor similar to the one we used above.

In such a case the high energy limits of the ratios considered in the above sections will lie between the values obtained in the above full compositeness case and the value 1 corresponding no mixing with $\phi = 0$.

5 CONCLUSIONS

In this paper we have shown that the assumption of t_R compositeness (while keeping t_L elementary) leading to suppressed $\gamma t_R t_R$ and $Z t_R t_R$ form factors at high q^2 , could immediately be checked by looking at the size of the cross sections and asymmetries of several basic production processes. The most spectacular changes with respect to the standard case are given by the following values of the ratios of new quantities (with t_R coupling suppressions) over standard ones: a factor 1/2 for the total unpolarized $e^-e^+ \rightarrow t\bar{t}$ cross section; a factor 3 for the longitudinal e^-e^+ polarization asymmetry as well as for its forward-backward asymmetry; a factor 1/2 for the gluon-gluon as well as for the photon-photon cross sections and for the neutral fusion process in e^-e^+ scattering.

The charged (WW) fusion process is more model dependent as it is very sensitive to the Higgs exchange contribution. We have illustrated two extreme cases where the ratio can vary from 1 to 0.2. In such a composite top model we noticed the possibility of a (very important) scale dependent top mass which has strong consequences in this WW

fusion process, in $bg \rightarrow tW_L^-$ and in other processes like $t\bar{t}H$ and $t\bar{t}Z_L$ production in e^-e^+ , photon-photon or gluon-gluon collisions where specific large reduction factors occur.

The above illustrations only correspond to arbitrary choices of compositeness effects with top form factors and a scale dependent effective top mass, but not to precise model predictions. We have only imposed the constraint that no effect (no anomalous coupling) should appear at low q^2 . In practice, in the case where departures from SM predictions would be observed at high energy in the considered processes, the following strategy could be applied. First, one should look precisely at the q^2 dependence of these departures, in order to see how they behave at high energy, in particular if the ratios tend to constant limiting values. Such precise observations could characterize the type of compositeness model responsible for these effects. One should then analyse the shape of these q^2 dependencies at intermediate energy and modelize them in terms of new physics constituent parameters, bound state wave functions, resonances etc. This would imply important works at future e^-e^+ , $\gamma\gamma$ and hadronic colliders.

After completion of our work, we were informed that a study of the effect of t_R compositeness at Tevatron and LHC through an effective four quark operator had been done in [22].

References

- [1] H. Terazawa, Y. Chikashige and K. Akama, Phys. Rev. **D15**, 480 (1977); for other references see H. Terazawa and M. Yasue, Nonlin.Phenom.Complex Syst. **19**,1(2016); J. Mod. Phys. **5**, 205 (2014).
- [2] D.B. Kaplan and H. Georgi, Phys. Lett. **136B**, 183 (1984).
- [3] K. Agashe, R. Contino and A. Pomarol, Nucl. Phys. **B719**, 165 (2005); hep/ph 0412089.
- [4] R. Contino, T. Kramer, M. Son and R. Sundrum, J. High Energy Physics **05**(2007)074.
- [5] G. Panico and A. Wulzer, Lect.Notes Phys. **913**,1(2016).
- [6] F. Richard, LAL-Orsay-1455, arXiv: 1403.2893 [hep-ph].
- [7] M. Fabbrichesi, M. Pinamonti and A. Tonerio, Eur. Phys. J. **C74**, 12,3193 (2014), arXiv: 1406.5393 [hep-ph].
- [8] G.J. Gounaris and F.M. Renard, Phys. Rev. **D92**, 053011 (2015); Phys. Rev. **D93**, 093018 (2016), arXiv: 1601.04142.
- [9] G.J. Gounaris and F.M. Renard, Phys. Rev. **D94**, 053009 (2016), arXiv:1606.08597.
- [10] F.M. Renard, Basics Of Electron Positron Collisions, Editions Frontières,1981.

- [11] D. Barducci, S. de Curtis, S; Moretti, G.M. Pruna, arXiv: 1504.05407 [hep-ph].
- [12] N. Kidonakis, arXiv: 1509.07848 [hep-ph].
- [13] S.D. Rindani *et al*, JHEP **1510**, 180 (2015); arXiv: 1507.08385 [hep-ph].
- [14] M. Beccaria *et al*, Phys. Rev. **D73**, 093001 (2006); arXiv: 0601175 [hep-ph].
- [15] B. Badelek *et al*, Int. J. Mod. Phys. **A19**, 5097 (2004), arXiv: 0108012[hep-ex].
- [16] M.S.Chanowitz and M.K. Gaillard, Phys. Lett. **B142**, 85 (1984); G.L. Kane, W.W. Repko and W.B. Rolnick, Phys. Lett. **B148**, 367 (1984); S. Dawson, Nucl. Phys. **B249**, 42 (1985).
- [17] R.P. Kauffman, Phys. Rev. **D41**, 3343 (1990).
- [18] M. Gintner and S. Godfrey, arXiv: 9612342 [hep-ph], eConf.0960625(1996)STC 130; C.-P. Yuan, Nucl. Phys. **B310**, 1 (1988).
- [19] M. Capdequi-Peyranere *et al*, Z. f. Phys. **C41**, 1988 (99).
- [20] A. Djouadi, J. Kalinowski and P. Zerwas, Z. f. Phys. **C54**, 1992 (255); H. Baer, S. Dawson and L. Reina, Phys. Rev. **D61**, 01302 (2000).
- [21] K.Hagiwara, H. Murayama and I. Watanabe, Nucl. Phys. **B367**, 1991 (267); U. Baur, A. Juste, L.H. Orr and D. Rainwater, Phys. Rev. **D71**, 054013 (2005).
- [22] Ben Lillie, Jing Shu, Timothy M.P. Tait, JHEP **0804**, 087 (2008), e-Print: arXiv:0712.3057; Kunal Kumar, Tim M.P. Tait, Roberto Vega-Morales JHEP **0905**, 022 (2009), e-Print: arXiv:0901.3808

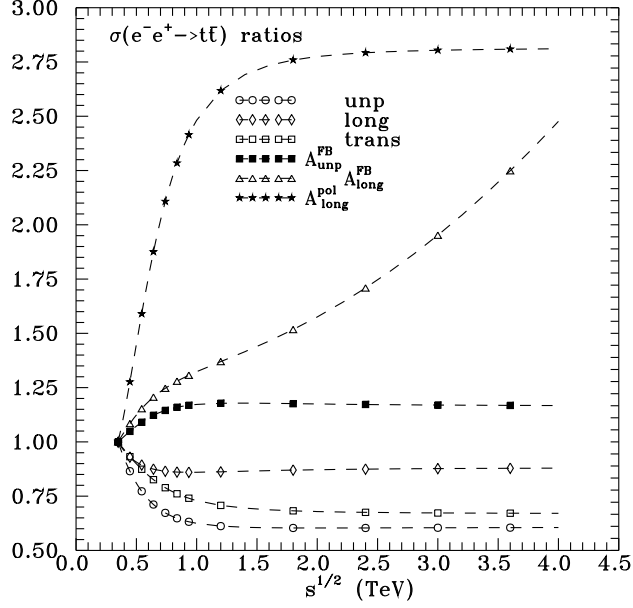


Figure 1: The energy dependencies of the ratios of the cross sections $\sigma(e^-e^+ \rightarrow \gamma, Z \rightarrow t\bar{t})$ with respect to the SM predictions, involving the g_{Vt}^R form factor effects of (2).

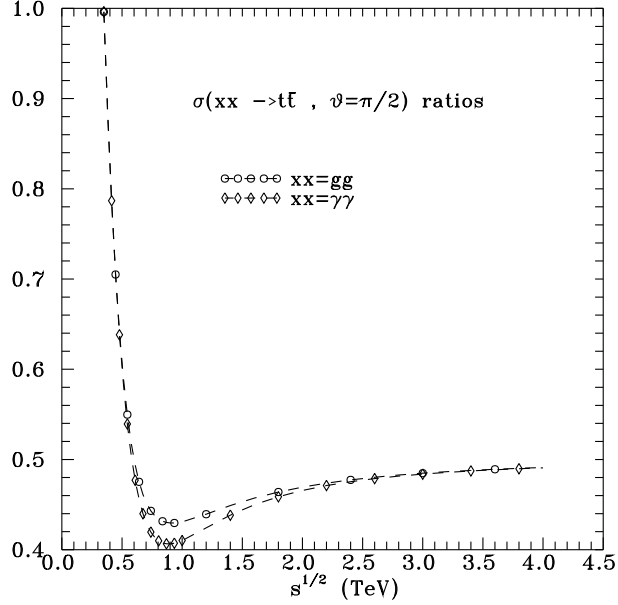


Figure 2: The energy dependencies of the ratios of the differential cross sections for $gg \rightarrow t\bar{t}$ and $\gamma\gamma \rightarrow t\bar{t}$ with respect to the SM predictions at $\theta = \pi/2$, involving the g_{Vt}^R form factor effects (2, 8).

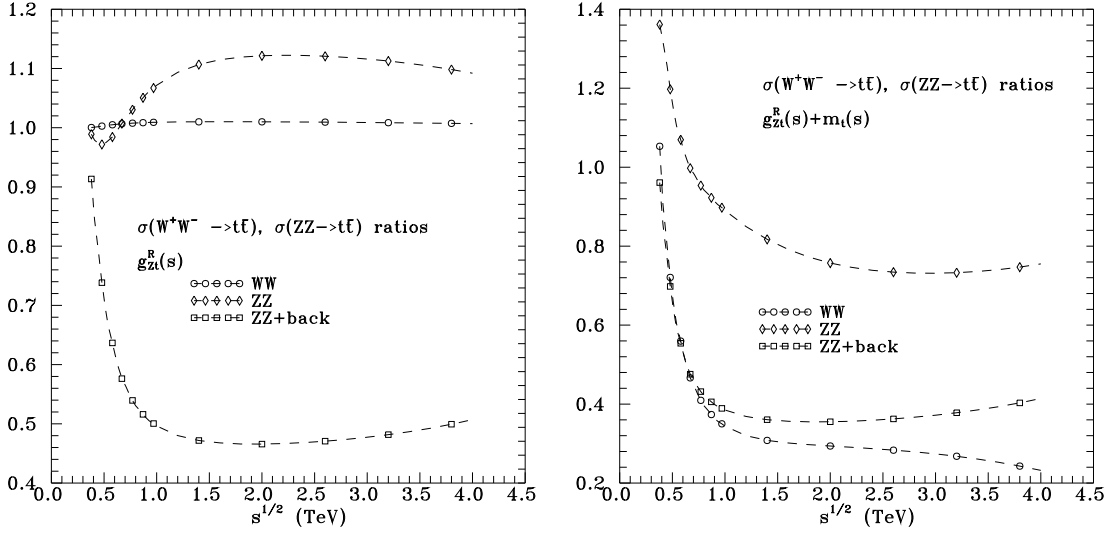


Figure 3: The energy dependencies of the ratios of WW , ZZ and $ZZ+\text{background}$ fusion cross sections, with respect to the SM predictions; see subsection 4.2. Left panel only contains the g_{Zt}^R effects (2, 8), while the right panel also includes the $m_t(s)$ effect of (12).

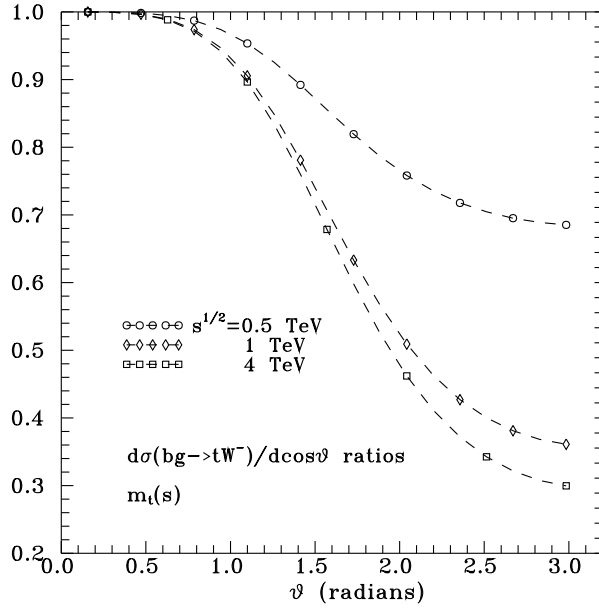


Figure 4: The angular dependencies of the ratios of the $bg \rightarrow tW^-$ differential cross sections, with respect to the SM predictions. The form factor effect only depends on $m_t(s)$ of (12).

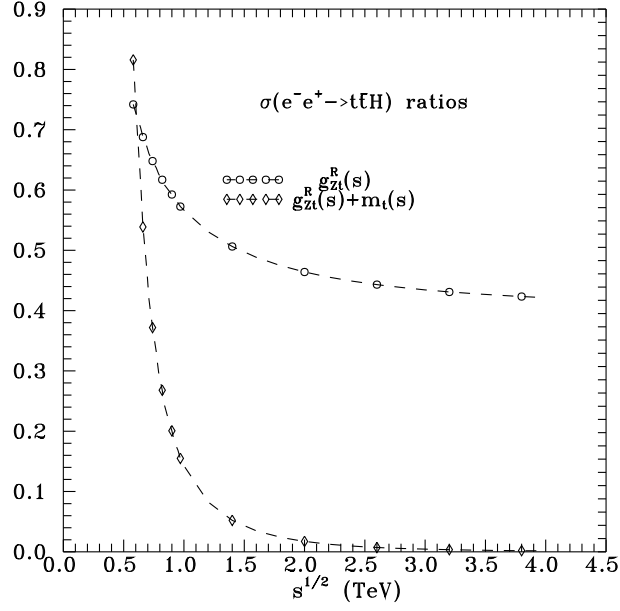


Figure 5: The energy dependencies of the ratios of the cross sections $e^-e^+ \rightarrow t\bar{t}H$, with respect to the SM predictions. The g_{Zt}^R and the $g_{Zt}^R + m_t(s)$ are obtained from (2, 8) and (12).

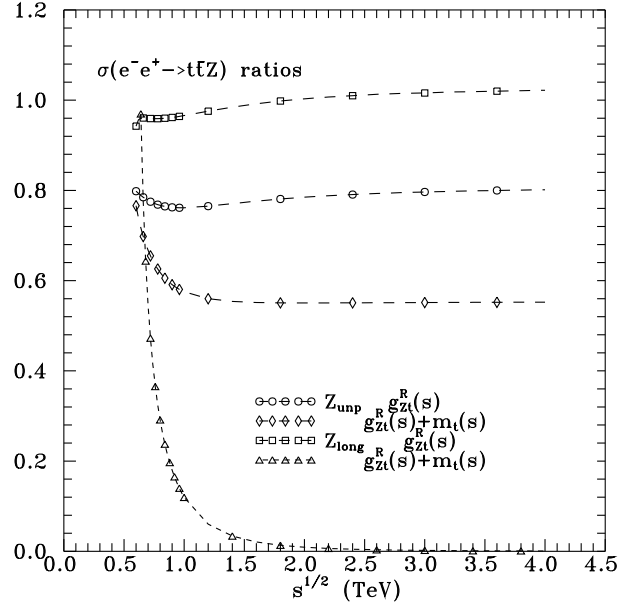


Figure 6: The energy dependencies of the ratios of the cross sections $e^-e^+ \rightarrow t\bar{t}Z$ for unpolarized Z , with respect to the SM predictions. The g_{Zt}^R and the $g_{Zt}^R + m_t(s)$ are obtained from (2, 8) and (12).

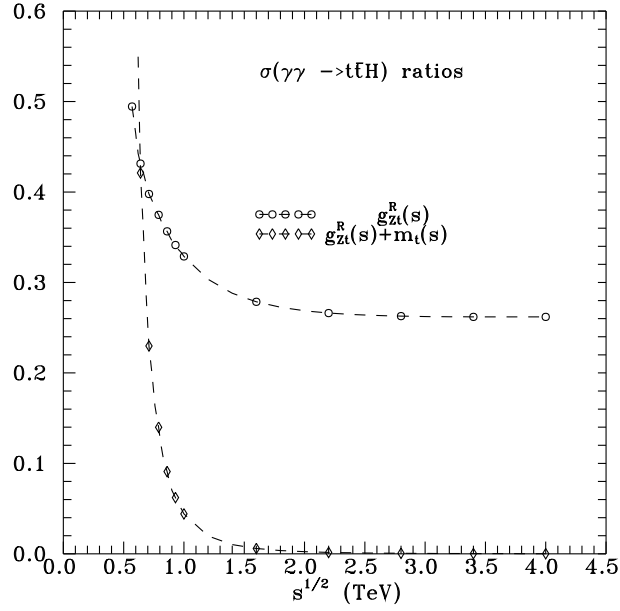


Figure 7: The energy dependencies of the ratios of the cross sections $\gamma\gamma \rightarrow t\bar{t}H$ with respect to the SM predictions. The g_{Zt}^R and the $g_{Zt}^R + m_t(s)$ are obtained from (2, 8) and (12).

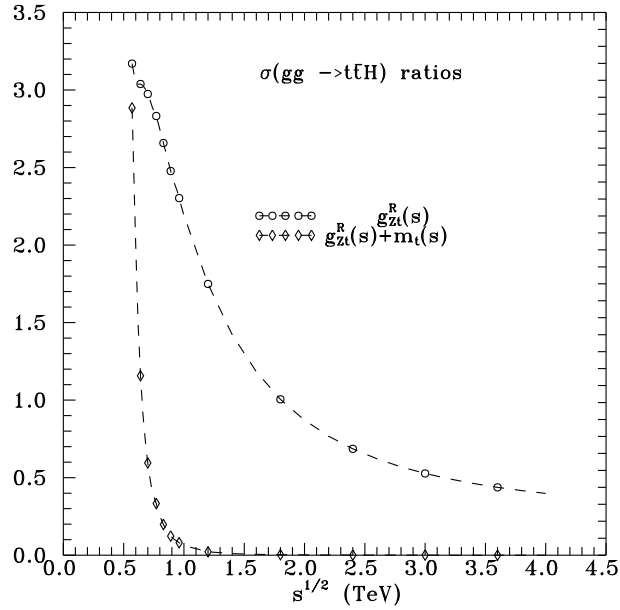


Figure 8: The energy dependencies of the ratios of the cross sections $gg \rightarrow t\bar{t}H$ with respect to the SM predictions. The g_{Zt}^R and the $g_{Zt}^R + m_t(s)$ are obtained from (2, 8) and (12).

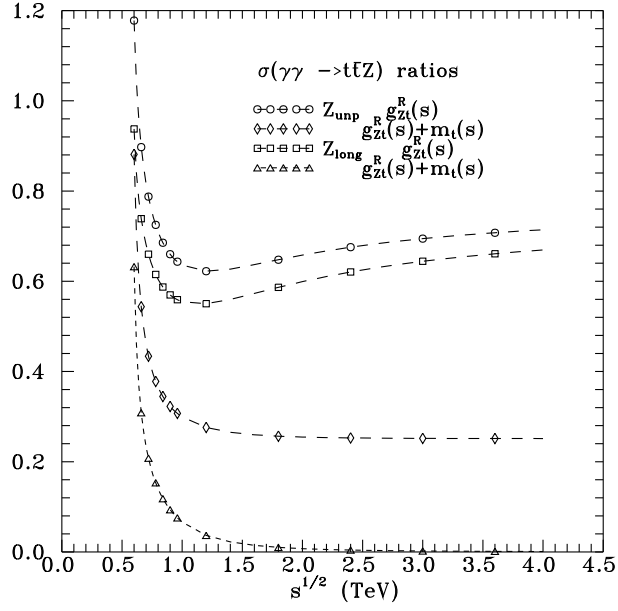


Figure 9: The energy dependencies of the ratios of the cross sections $\gamma\gamma \rightarrow t\bar{t}Z$ for unpolarized Z , with respect to the SM predictions. The g_{Zt}^R and the $g_{Zt}^R + m_t(s)$ are obtained from (2, 8) and (12).

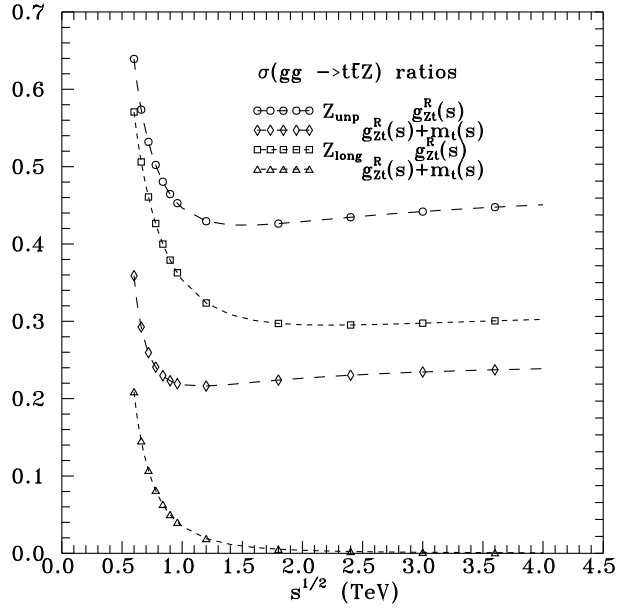


Figure 10: The energy dependencies of the ratios of the cross sections $gg \rightarrow t\bar{t}Z$ for unpolarized Z , with respect to the SM predictions. The g_{Zt}^R and the $g_{Zt}^R + m_t(s)$ are obtained from (2, 8) and (12).